ELSEVIER

Fusion Engineering and Design 42 (1998) 281–288

Fusion Engineering and Design

The use of MNCP for neutronics calculations within large buildings of fusion facilities

J.E. Eggleston *, M.A. Abdou, M.Z. Youssef

Mechanical and Aerospace Engineering Department, UCLA, Los Angeles, CA 90095, USA

Abstract

The calculation of nuclear parameters within fusion facilities is complicated by the complex geometry and large size of the proposed buildings housing the reactors. These complications make it impossible to use a single model, or code, to calculate the transport of neutrons from the plasma out into the rest of the building. In this paper, coupling two calculational models is demonstrated in calculating the operational dose rates in ITER building. The neutron and gamma fluxes during operation are calculated from the plasma region out to the cryostat of the machine using a two-dimensional discrete ordinates model (the subject of a companion paper) whereas a Monte Carlo MCNP model is applied in the rest of the building. In using this coupling approach, numerous joint Probability Mass Functions (PMFs) for the different phase space variables are used and constituted a specially-written source subroutine that is linked to MCNP. Along with the problem of proper source sampling and characterization, the physical size of the building, in comparison to the tally region, drastically complicates the calculation. As a result of this, the use of non-analog techniques are needed to help in the transport of particles in regions far away from the source (which is the NBI duct in this case). The fact that good results were easily achieved in the NBI room where there is a direct line of sight to the plasma, but as the detectors are placed further away, the results degenerate, exemplifying the need to use variance reduction techniques. Various techniques in the MCNP calculations are applied and compared and their usefulness is discussed. It is shown that MCNP can be used, in a limited fashion, to focus on specific high importance regions within large buildings such as in ITER.

1. Introduction

The calculation of the biological dose within fusion facilities is complicated both by the complex geometry and large size of the proposed reactor buildings. While neutronics codes and computers have become much more powerful over the years, they are still inadequate to fully model large complex systems. Fusion reactors, such as the machine proposed for ITER, are very large with much material between the neutron source (the plasma) and the biological shields (located tens of meters away). The reactor facility, by its very nature, is also large and optically thick. This prevents the use of a single model or code to treat the entire system of machine and building. As a result of this, numerous models and codes must be used, requiring them to be coupled together via the angular flux at carefully chosen locations.

* Corresponding author.

0920-3796/98/$19.00
PII S0920-3796(98)00215-4

Discrete ordinates method, the most widely used deterministic approach, calculates and stores the entire span of phase space. Although this allows for the easy calculation of any nuclear response, it becomes computationally expensive, both in computer time and storage requirements, when multidimensional models are solved. To keep the computational size of the problem to a minimum, the discretization of phase space must be kept sparse. Very large spatial, energy, and angular discretizations must be used which hurts the accuracy of the results generated by these codes [1]. However, stochastic methods, like MCNP [2], do not need to discretize phase space, but treats it as a continuum, this creates a large reduction in the storage needed to run large problems, and complicated three-dimensional geometries can easily be modeled. This fact is what makes stochastic methods attractive for geometrically complicated problems. However, the probabilistic nature of the codes makes a detailed mapping of phase space in geometrically large and optically thick problems prohibitively expensive, and as such only specific regions can be focused on for a given calculation.

There have been numerous studies to calculate the nuclear response in a fusion environment in the past. Many of these studies were for the operation of the TFTR machine at Princeton [3–6]. These papers give a very good discussion on useful methods when doing neutronics calculations in complicated systems. However, the TFTR has little shielding and a high leakage rate for neutrons and gamma rays that are generated within the plasma which allows for the straightforward use of MCNP. This is not the case for ITER with its high neutron yield and its large amount of shielding between the plasma and the building. Here, MCNP has been used to calculate integrated nuclear responses within the machine itself and not within the larger volume of the building [7,8]. The large increase in size and shielding for the ITER machine requires one to reinvestigate the usefulness of MCNP for such problems. This paper discusses the coupling methods, inherent problems, and techniques that can mitigate these problems when MCNP is used to calculate the transport of neutrons through a large optically thick problem. To act as a focal point, the biological dose found within the proposed ITER facility during reactor operation is analyzed here.

To begin, the neutron and gamma ray fluxes are calculated from the plasma region out to the cryostat of the machine using a two-dimensional discrete ordinates model developed for DORT [9,10]. An MCNP model of the building was then coupled to the discrete ordinates model at the cryostat, where many of the symmetry assumptions that went into the formulation of the 2-D model break down. The transport is then continued throughout the building. The following sections discuss the coupling methodology used between these two codes, the variance reduction techniques and their effectiveness, and, finally, the MCNP model and the actual dose rates found at specific locations within the building.

2. Coupling methodology

The coupling of a discrete ordinates code to a stochastic code requires that the calculated angular flux at the desired location, i.e. the cryostat, be transformed into PMFs for the different phase space variables of the source particle. A special source subroutine is then linked to MCNP that uses these PMFs to generate the source for the building model. The order of choice for the starting particles, and their level of dependence is that the position is free to be chosen, then the energy is given its position, and then the direction is given its position and energy. Thus the order of selection, and the particles level of dependence is: Position → Energy → Direction.

The angular flux, at the desired locations, is stored in a BNDRYS formatted file. A code, named PROBGEN was written to interface with this file and use the equations given here to generate the necessary PMFs for the source particles in the MCNP calculation. The starting position is the first layer of dependence in this coupling scheme. Since the machine model is 2-D [10] $\{R–Z\}$, only the axial position for a fixed R can be defined through the angular flux; the planar coordinates $\{X$ and $Y\}$ must be chosen randomly

such that they are confined to the surface of the cryostat. The probability of any spatial bin[1] along the z-axis, $p(Z_i)$, is based on the ratio of the total number of particles crossing at that location to the total number of particles crossing the entire surface of the cryostat. Mathematically this is given by:

$$p(Z_i) = \frac{\Sigma_{g=1}^{IGM} \Sigma_{j=1}^{MM} w_j \phi(Z_i, \Omega_j, E_g) A_i}{\Sigma_{i=1}^{IM} \Sigma_{g=1}^{IGM} \Sigma_{j=1}^{MM} w_j \phi(Z_i, \Omega_j, E_g) A_i} \quad (1a)$$

Where $\phi(Z_i, \Omega_j, E_g)$ is the angular flux at the cryostat, E_g is the energy of group 'g' (total number of energy groups is IGM), Ω_j is the direction 'j' with quadrature weight w_j (total number of directions is MM), and A_i is the area of Z_i spatial bin at the cryostat (total number of spatial bins is IM). The probabilities calculated by Eq. (1a) are then used, in conjunction with a random number ξ, to choose the axial spatial bin such that bin I is chosen when:

$$\Sigma_{i=1}^{I-1} p(Z_i) \leq \xi \leq \Sigma_{i=1}^{I} p(Z_i) \quad (1b)$$

The final value of Z is then randomly sampled from within this bin by choosing another random number ξ' and defining Z by:

$$Z = Z_I + \Delta Z_I^* \xi' \quad (1c)$$

In a similar fashion the energy's joint PMF is defined by the following expression:

$$p(E_g \backslash Z_I) = \frac{\Sigma_{j=1}^{MM} w_j \phi(Z_I, \Omega_j, E_g)}{\Sigma_{g=1}^{G} \Sigma_{j=1}^{MM} w_j \phi(Z_I, \Omega_j, E_g)} \quad (2)$$

Where $p(E_g \backslash Z_I)$ is understood to be the probability of E_g given Z_I. The energy bin G is chosen analogous to Eq. (1b) and the final value of E is calculated in the same fashion as Eq. (1c). The resulting PMFs are given in Fig. 1a,b. It is interesting to note that the ray effect, which is one of the major problems with the use of discrete ordinates in streaming problems [1], is clearly seen in the PMF distribution for neutrons. The double prong shape of the 14 MeV peak directly corresponds to the discrete nature of the directions that the neutrons are allowed to stream down. This acts to increase the flux, and the PMF, at the edges of the NBI duct (which is centered at $Z = -1973.5$ cm). The gamma rays PMF does not show this behavior since the gamma rays are generated volumetrically by the interaction of the neutrons with the material of the machine and, as such, the ray effect is washed away.

The treatment of the particle direction is handled in a similar way to position and energy. A joint PMF table, $p(\Omega, E \backslash Z_I)$, is created in an analogous way to Eq. (1a) and Eq. (2):

$$p(\Omega_j, E_g \backslash Z_I) = \frac{w_j \phi(Z_I, \Omega_j, E_G)}{\Sigma_{j=1}^{MM} w_j \phi(Z_I, \Omega_j, E_G)} \quad (3)$$

Eq. (3) defines the probability for every angle used in the discrete ordinates method. That is, if the machine calculation used an S6 quadrature scheme, then there would be 30 probabilities, each corresponding to a unique direction. The angular bin selection was conducted in the same fashion as shown in Eq. (1b), and the final direction was sampled randomly from within the selected bin. It must be noted that care was taken to insure that the angle chosen was translated out of the 2-D R–Z model geometry into the 3-D MCNP model geometry.

A special source routine was written and linked to MCNP to interpret the probability tables and follow the steps outlined above. The routine utilizes a pseudo-random number generator routine within MCNP to generate the needed random numbers. Eq. (1b) and Eq. (1c) are used to set the source particles starting values.

3. ITER Building model and results

The MCNP model developed for the building was a 180° segment which included the discrete NBI and diagnostic ports in the NBI Hall as seen in Fig. 2. The model was designed to analyze the angular variation of integrated nuclear responses as one moves around the machine in the NBI Hall and the Pit Gallery located directly behind the NBI Hall. The tallies used were F2 surface tallies that estimated the flux and dose on both sides of the pit wall (A and B in Fig. 2a,b). For the dose calculations, the flux to dose conversion factors given in Battat [11], and plotted in Fig. 3, were

[1] A bin is defined as the difference between two adjacent discrete points, in this case spatial points.

used. Note that both the neutron and gamma flux to dose conversion factors are smooth functions of energy; this helps to keep the tallies fairly well behaved and leads to a faster convergence of the solution. If the nuclear response sought was not smooth in energy, but had numerous resonance regions, then the relative error in the calculated response would become ill-behaved and converge very slowly.

Fig. 4 shows the toroidal dependence of the total dose rate during operation in, μSv h^{-1} within the Equatorial NBI Hall and the Pit Gallery located behind. (Regions A and B in Fig. 2). The stainless steel shield doors reduce the dose by about three orders of magnitude (changing the dose rate from 10^6–10^3 μSv h^{-1} in the Pit Gallery, and 10^{12}–10^9 μSv h^{-1} in the NBI Hall) as one moves around the machine. The pit wall decreases the dose by roughly six orders of magnitude. Also, the neutron's contribution to the dose is no longer dominates as one moves from the NBI Hall to the Pit Gallery behind it, but the neutron produced gamma rays become dominant in the Pit Gallery (γ contribution in the NBI Hall ranges between 5–9% and in the Pit Gallery it ranges between 85–95%). The increase in the gamma dose is a direct response to the n-γ reactions that occur in the steel within the concrete walls. (For a detailed description of the material compositions used in the model please refer to Youssef [10]).

These results are consistent with Youssef [10] who did a fairly extensive 2-D and 3-D dose rate calculation for the ITER building using the discrete ordinates method. Although the results are consistent, in general, the inherent problems with the discrete ordinates method were not seen using MCNP. The ray effect which is evident when discrete ordinates is used to follow particles through ducts is not evident in the integrated dose distribution shown in Fig. 4. The dose at the front of the pit wall is fairly smooth and constant in the toroidal direction as well as along z. The reason is because of the continuous sampling method described earlier, and because the results are averages over discrete areas on the surface and not point values as the discrete ordinates method gives. Both of these reasons act to mitigate the ray effect. The inherent size of the problem requires that the tally regions be large, making the results to be a course dose map of the building and not a point by point mapping that the discrete ordinates method can generate. This shortcoming is more than made up for by the capabilities of MCNP to accurately model the problem geometrically and treat the energy dependence continuously.

4. Observations on variance reduction applied to the building model

Three variance reduction techniques were studied to see if any improvement in the relative error

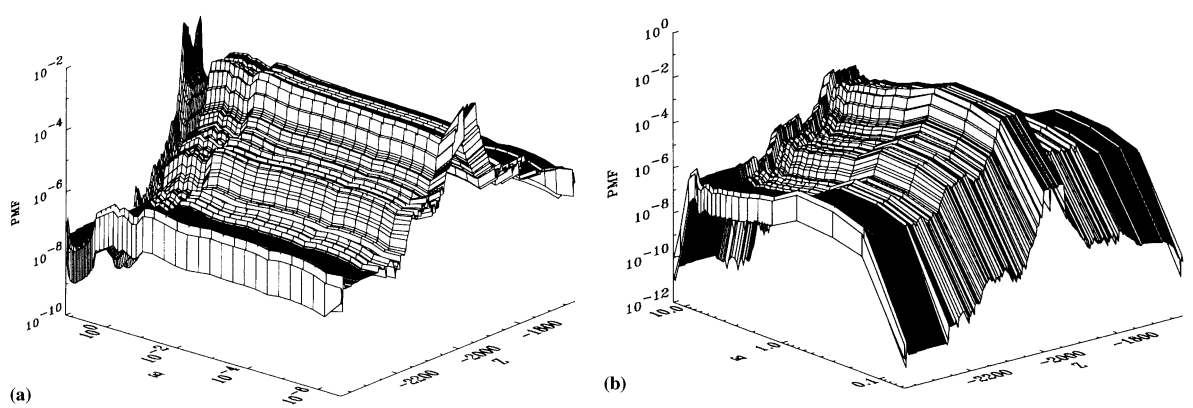

Fig. 1. (a) The joint PMF, $p\,(E_g \backslash Z_I)$, for neutrons. (b) The joint PMF, $p\,(E_g \backslash Z_I)$ for gamma rays. E is in MeV and Z is in cm. Note the increase in probability for all energy neutrons and gamma rays at $Z = 2{,}000$ cm, the location of the NBI ports.

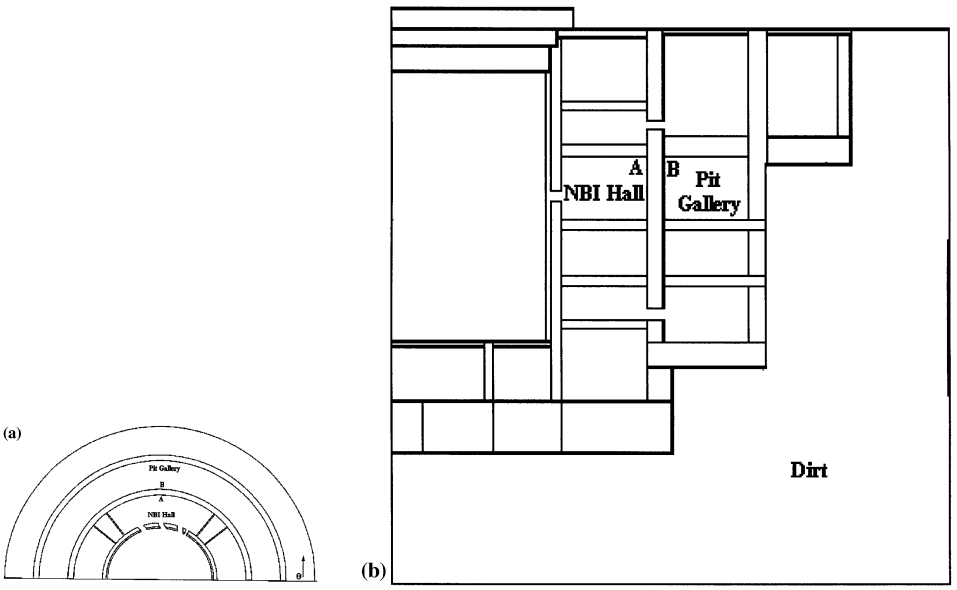

Fig. 2. (a) X-Y view of the MCNP building model at the equatorial level ($Z = -20$ m). (b) Y-Z view of the MCNP building model. Note, A and B in the NBI Hall and Pit Gallery are the locations of the tally surfaces.

or computation time could be achieved. The techniques used were weight windows, exponential transform, and weight cutoff. Using variance reduction techniques is important because the variance, $S_{\bar{x}}^2$, directly relates to the relative error, R, by $R \equiv S_{\bar{x}}/\bar{x}$, where $\bar{x}$ is the average of the nuclear response x. The effect of the weight windows is to decrease $S_{\bar{x}}^2$ by confining the weight to be within a specified window of allowed weight (see Briemeister [2] for a detailed discussion of the theory behind the use of weight windows, the exponential transform, and weight cutoff). The weight window lower bound was energy independent and defined to decrease by an order of magnitude each time the flux decreased, and the upper bound was defined to be five times the lower. This is achieved by setting the width for any given cell within the shields and walls equal to the average mean free path of neutrons. For neutron energy greater than 10 MeV the mean free path is ~ 10 cm and hence the biological shield and pit walls were segmented into cells of ~ 10 cm widths with the window lower parameter decreasing by a factor of 3–8 for each cell the neutrons would cross moving away from the cryostat. The weight cut off was used in conjunction with this to decrease the computer time used to track very low weight particles. The lost value, or weight, of the particles is then stochastically added to the weight of other particles within the same cell to

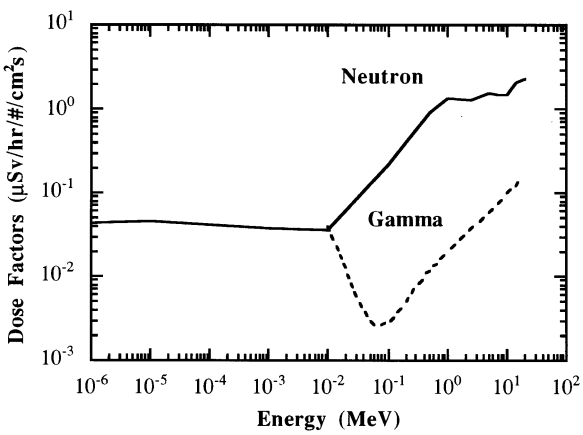

Fig. 3. The neutron and gamma flux to dose conversion factors used in the calculation. Note that the gamma factors only go as low as 0.01 MeV (values taken from Battat [11]). The smooth shape of the factors improves the statistical convergence of the dose calculations.

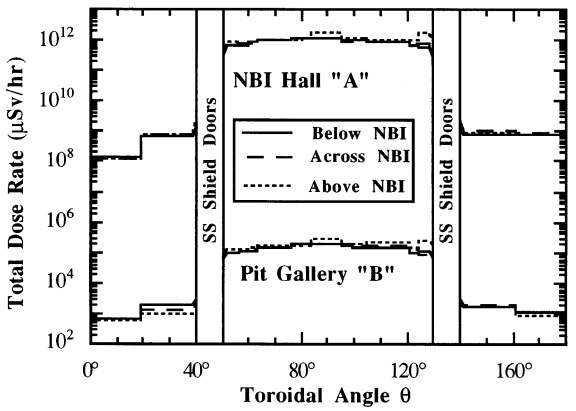

Fig. 4. Toroidal variation of the total operational dose rate for regions below, across, and above the NBI ports within the NBI Hall, A, and Pit Gallery, B.

ensure that the problem is not inadvertently biased.

The exponential transform reduces R by increasing the number of particles that actually reach the tally region of a model. It is easily shown that $S_{\bar{x}} \sim 1/\sqrt{N}$ [12] and as such that $R \sim 1/\sqrt{N}$. The exponential transform adjusts the cross sections of a material and the weights of the particles to encourage their transport in a desired direction without statistically biasing the problem. For the building model, the direction was chosen such that the particles would preferentially move radially outwards when inside the pit wall and radially inwards from outside the pit wall to where the tally surfaces are located. The transform parameter, the fractional amount the cross sections and weight are modified [2], was set at 0.7 for neutrons and 0.9 for gamma rays.

The two techniques are compared to each other on how well they reduce R and if they have significantly increased computation times. Fig. 5 compares the relative errors for these methods, for both neutrons and γs as a function of the toroidal angle defined in Fig. 2a. Note that the γ relative error is divided by 5 to keep the figure uncluttered. On the average, the neutron dose R shows negligible improvement when using the exponential transform. The percent decrease is as high as 40% (at a θ of 76°) and the percent increase is as high as 40% (at a θ of 80°) with a general overall worsening of the relative error with its use. This indicates that it is not the number of particles that reach the tally region, but the variance in the weight of the neutrons that dictate the relative error in the integrated dose. Thus, for a fixed number of particles (NPS = 500000 for neutrons) it is not the increasing of the number that reach the tally regions, but the variation in the weight of these particles that has the most significant impact on the relative error. When the exponential transform was used there was a 211% increase in the total number of particles in the Pit Gallery for the NBI Hall. Although the exponential transform dramatically increased the number of neutrons reaching the tally region, with an increase in the computation time of 15%, it was not enough to offset the increase in the particles weight variation caused by the exponential transform. The end result was to increase the computation time while having little effect on the relative error of the nuclear response.

The gamma dose R, shows a general improvement when the exponential transform is used (as seen in Fig. 5). Compared to the weight windows variance reduction technique, the percent decrease ranges from 3 to 45 with an increase near the region behind the shielding doors of $\sim$38%. Whereas the neutron relative error truly oscillated between decreasing and increasing values of R, the photon R showed a consistent improvement in

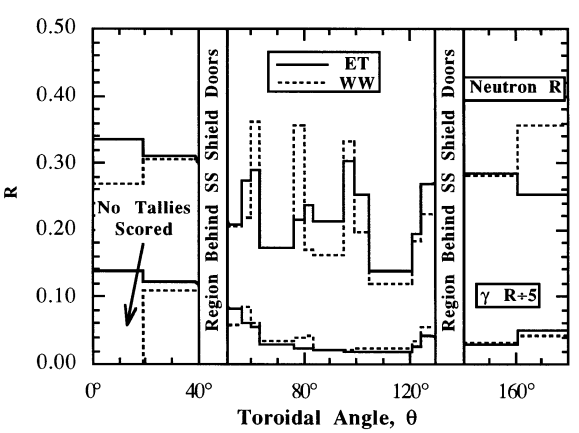

Fig. 5. The toroidal variation of the relative error, R, for the operational neutron and gamma dose rates. The exponential transform has helped to reduce R overall for the gamma rays, but had mixed results for the neutrons.

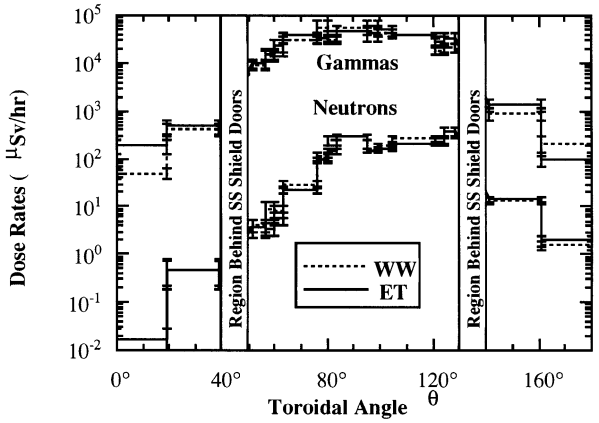

Fig. 5. The toroidal variation of the relative error, R, for the operational neutron and gamma dose rates. The exponential transform has helped to reduce R overall for the gamma rays, but had mixed results for the neutrons.

the region directly behind the NBI Hall. This indicates that for a fixed number of particles from the sampling source (NPS = 2000000) it is the number of photons that reach the tally surfaces that have the overriding effect on the relative error and not the variation in the weight of the particles that the exponential transform creates. The exponential transform increased the number of particles in the Pit Gallery for the NBI Hall by 187% and decreased the computation time by 4.67%. Also note that whereas the weight windows had a region where no tallies scored, near 0° in Fig. 5, the exponential transform had scores in all tally regions. Fig. 6 shows the dose rate for both the neutrons and the machine produced gamma rays. It is apparent from studying this figure that the exponential transform does not add any apparent bias to the calculation. Both weight windows and exponential transform results fall within the statistical error limits of each other except for the neutron dose near 0°. This is where the statistical errors were the highest and the results become somewhat suspect. It can be concluded that it is beneficial to use exponential transforms for gamma transport through the ITER building, but it does not have any apparent benefits for its use for neutron transport.

5. Conclusions

This work has shown that MCNP can indeed be used in a limited fashion to calculate the nuclear response within large volume, optically thick problems. The speed of solution depends on the type of nuclear response desired. For reactions that do not contain resonances within the desired energy range, i.e. biological dose, the solution converges fairly quickly. The results calculated can give insight into the three-dimensional behavior of the nuclear response within the ITER building. By carefully choosing the dimension of individual cells within the problem to be on the order of the particle mean free path, choosing the weight window lower bound to decrease by a factor of e as one moves away from the cryostat, and using exponential transforms for the gamma rays, an accurate $R–Z–\theta$ calculation can be done within a short time frame ($\sim$1 week or less) without worrying about prohibitively large memory storage requirements. Thus, MCNP, after a careful study of the nuclear physics of the problem and a careful choice of the nuclear response desired, can be used to map out a given response with some degree of success for optically thick and geometrically large problems.

Acknowledgements

The authors wish to thank C.W. Barnes of Los Alamos National Laboratory for the use of the computational resources at his disposal and A. Kumar for many useful discussions on MCNP coupling.

References

[1] E.E. Lewis, W.F. Miller, Computational Methods of Neutron Transport, Wiley, New York, 1984.
[2] J.F. Briesmeister, MC NP-4A general Monte Carlo N-particle transport code, Technical Report LA-12625-M, Los Alamos National Laboratory, 1993.
[3] L.P. Ku, J.G. Kolibal, S.L. Liew, A comparison of 1-,2-, 3-dimensional modeling of the TFTR for nuclear radiation transport analysis, Technical Report PPPL-2244, Princeton Plasma Physics Laboratory, 1985.

[4] S.L. Liew, L.P. Ku, J.G. Kolibal, Three-dimensional Monte Carlo calculations of the neutron and γ-ray fluence in the TFTR diagnostic basement and comparisons with measurements, Technical Report PPPL-2275, Princeton Plasma Physics Laboratory, 1985.

[5] S.L. Liew, J.G. Kolibal, L.P. Ku, Shielding analysis of the major labyrinths in the TFTR test cell, Technical Report EAD-R-27, Princeton Plasma Physics Laboratory, 1984.

[6] A. Kumar, M.A. Abdou, J.E. Eggleston, H.W. Kugel, G. Ascione, S. Elwood, Measurement and calculation of doses in and around north-west labyrinth in TFTR test cell shielding for D-T operation, Proc. 16th IEEE/NPSS Symp. Fusion Engineering, Champain, Illinois, USA, October 1995.

[7] M.E. Sawan, Y. Gohar, R. Santoro, Shielding analysis for the ITER divertor and vacuum pumping ducts, Fusion Eng. Des. 28 (1995) 429–436.

[8] S. Sato, H. Takatsu, Y. Seki, T. Utsumi, Streaming analysis of gap between blanket modules for fusion experimental reactor, Fusion Technol. 30 (1996) 1129–1133.

[9] W.A. Rhodes, TORT-DORT, Two and three-dimensional discrete ordinates transport code, Technical Report CCC-543, Radiation Sheilding and Information Center, RSIC, Oak Ridge National Laboratory, 1992.

[10] M.Z. Youssef, et al., Assessment of dose rate profiles during operation and after shutdown inside the building of the experimental fusion reactor, Fusion Eng. Des. 42 (1998) 155–172.

[11] ANS-6.1.1 Working Group, M.E. Battat (Chairman), American national standard neutron and gamma-ray flux-to-dose rate factors, ANSVANS-6.1.1-1977 (N666), American Nuclear Society, La Grange Park, Illinois, 1977.

[12] A.H-S. Ang, W.H. Tang, Probability Concepts in Engineering Planning and Design. Volume 1: Basic Principles, Wiley, New York, 1975.